Collisional diffusion in a two-dimensional point vortex gas or a two-dimensional plasma

Daniel H. E. Dubin
Department of Physics, University of California at San Diego, La Jolla, California 92093

(Received 20 November 2002; accepted 7 February 2003)

This paper analyzes collisional diffusion of a multispecies two-dimensional (2D) point vortex gas, or a 2D plasma, in the presence of retrograde shear. Diffusion both along and across the shear flow is calculated using Boltzmann, Kubo, Klimontovitch and resonance-broadening theories. It is shown that diffusion is reduced in the presence of shear, just as for the shear reduction of transport observed in fusion plasmas. Here, however, fluctuations are thermal rather than turbulent, allowing a rigorous calculation of the transport. When there are several species of point vortices, Onsager relations require that the diffusive flux conserves the total vorticity $\rho(r)$, which is proportional to charge density in the plasma analogue. Surprisingly, the diffusive flux *concentrates* vortices with large positive (or negative) circulations at maxima (or minima) of the mean vorticity profile. © *2003 American Institute of Physics.* [DOI: 10.1063/1.1564596]

I. INTRODUCTION

The two-dimensional (2D) point vortex gas is a useful paradigm for more complex fluid flows, and has been successfully applied to the study of 2D Euler flow,[1] fluid turbulence,[2–5] and transport in neutral[6–8] and non-neutral plasmas.[9] This paper considers the diffusion of a multispecies point vortex gas, focusing on the effect that an applied stable shear flow has on the diffusion.

Using kinetic theory based on Boltzmann, Kubo, and Klimontovitch approaches, we show that the diffusion is reduced in the presence of applied retrograde velocity shear. This result is similar to the shear reduction of transport observed in fusion plasmas.[10] Here however, the fluctuations are assumed to be thermal, rather than turbulent, and consequently the resulting shear reduction of the transport can be calculated rigorously.

The point vortex gas has relevance to magnetized plasmas due to the well-known isomorphism between the dynamics of an ideal incompressible 2D fluid, described by the Euler equations, and the dynamics of a guiding-center plasma of charged rods undergoing 2D $\mathbf{E}\times\mathbf{B}$ drift dynamics.[11] The ith charged rod, with charge q_i per unit length, is equivalent to a point vortex with circulation

$$\gamma_i = -\frac{4\pi c}{B} q_i , \tag{1}$$

where B is the magnetic field strength and c is the speed of light. Also, the electrostatic potential $\phi(r)$ is related to the stream function $\psi(r)$ by $\psi = c\phi/B$.

Our results thus apply directly to experiments that measure collisional diffusion in cylindrical non-neutral plasma columns. Such columns rotate with an $\mathbf{E}\times\mathbf{B}$ rotation frequency $\omega(r) = V_\theta(r)/r$ that can have substantial radial shear. We therefore focus our attention on cylindrically symmetric flows characterized by a shear rate $S(r) \equiv r\,\partial\omega/\partial r$. For an electron column with $\gamma_i > 0$, a monotonically decreasing density $n(r)$ gives a retrograde flow with $\gamma_i S < 0$.

Taylor and McNamara previously considered the collisional diffusion of a homogeneous, *shear-free*, 2D guiding center plasma as a possible model for anomalous transport in fusion plasmas.[7] In this seminal work, the authors obtained the diffusion coefficient of a ''test'' point vortex, assuming that the distribution of vortices is random and uncorrelated, as

$$D^{\mathrm{TM}} = \frac{1}{2}\frac{c}{B}\sqrt{\sum_{i=1}^{N}\frac{q_i^2}{\pi}} = \frac{1}{8\pi}\sqrt{\sum_{i=1}^{N}\frac{\gamma_i^2}{\pi}}. \tag{2}$$

Equation (2) exhibits two important properties: first, the diffusion scales as $1/B$, in agreement with the semiempirical Bohm-scaling law. Second, the diffusion coefficient is not intensive, but rather increases in proportion to the system size R, since $N \propto R^2$. This is because the diffusion is dominated by large-scale fluctuations (Dawson–Okuda vortices[8]) whose size is of order R. The Coulomb interaction is inherently long-range, and ''collisions'' can occur with arbitrarily large impact parameters; these long-range $\mathbf{E}\times\mathbf{B}$ drift collisions are quite distinct from the short-range velocity-scattering collisions normally considered in plasma physics.

The Dawson–Okuda vortices are simply fluctuations in the local vorticity, i.e., fluctuations in the charge density. A portion of the system containing roughly N_e point vortices, each with circulation γ, might be expected to have a fluctuation in the circulation of order $\gamma\sqrt{N_e}$. Such a fluctuation is a locally rotating eddy that turns over in a time of order $\Delta t_e = R_e^2/\gamma\sqrt{N_e}$, where R_e is the size of the eddy; the eddy presumably dissipates in a time Δt_e. The macroscopic diffusion is caused by a sequence of these random fluctuations, with step size R_e and correlation time Δt_e. This gives the scaling of Eq. (2), as $D^{\mathrm{TM}} \sim R_e^2/\Delta t_e \sim \gamma\sqrt{N_e}$.

However, Eq. (2) neglects all correlations between the point vortices. One expects Debye shielding to limit the maximum size of eddies to a Debye length λ_D. In this case the diffusion is reduced to roughly $D^{\mathrm{TM}}\lambda_D/R_e$.[7,8]

In this paper we consider the effect that stable shear flow has on the Taylor–McNamara diffusion in a cylindrical vortex patch of overall radius R, consisting of N point vortices. The shear flow destroys the largest Dawson–Okuda vortices, and greatly reduces the diffusion compared to Eq. (2). A previous paper analyzed the radial diffusion for N identical point vortices, and also compared the theoretical results to simulations of the radial diffusion.[9] Here, we generalize the theory in several respects. First, we consider a system consisting of several species. Diffusion coefficients $\overline{D}_{ab}$ for the diffusion of species a due to gradients in the density of species b are derived, and are shown to obey Onsager relations. The overall evolution of the system under the action of these diffusive fluxes is considered. The Onsager relations imply that the diffusive flux conserves the total vorticity profile $\rho(r)=\Sigma_a \gamma_a n_a(r,t)$, where $n_a(r)$ is the number of vortices of species a per unit area.

Thus, the diffusive fluxes cannot drive the system to a thermal equilibrium state, in which vorticity ρ is related to the stream function ψ by $\rho=Ce^{\beta\psi}$, with C a constant and β the inverse temperature. Instead, the system approaches a thermal equilibrium state only if the effects of viscosity are taken into account. The viscosity of a sheared point-vortex gas was analyzed previously, and calculated for the case of nonmonotonic $\omega(r)$, but is still an active area of research.[12] We will see that the diffusive fluxes do increase an entropy functional. Surprisingly, these fluxes cause point vortices with large positive circulations to concentrate in regions of maximum average vorticity, and vortices with large negative circulation to concentrate at vorticity minima [without changing the total vorticity profile $\rho(r)$, however]. This counter-intuitive vorticity concentration is closely related to the macroscopic motion of a vorticity clump up a background gradient or a vorticity hole *down* a background gradient.[13–15]

Other authors[16–18] have also considered the diffusion of vorticity in both turbulent and thermal 2D Euler flow, and have come to similar conclusions concerning the relation between diffusion and gradient-driven drift. However, Refs. 16 and 18 associate this drift with a *mobility* flux caused by the gradient not in the vorticity, but in the stream function. This is correct only if the vorticity is already related to the stream function through the Boltzmann distribution. Unfortunately, the authors use this mobility form for the drift to mistakenly conclude that diffusion and mobility can drive the system to a global thermal equilibrium state, even for a single species system. Since thermal equilibrium was already assumed, their analysis cannot be employed to understand the approach to thermal equilibrium.

Finally, we evaluate the diffusion along the direction of the shear flow (the θ direction). We find that vortices experience superdiffusion in the θ direction as they are swept away by the shear flow.

II. BOLTZMANN ANALYSIS OF CLOSE COLLISIONS

In this section, we analyze the vortex motion during isolated two-vortex collisions. This analysis applies to vortices whose separation is small compared to an average interparticle spacing. Consider two vortices, at positions $\mathbf{r}_a$ and $\mathbf{r}_b$, with circulations γ_a and γ_b, respectively. The vortices interact as they are carried along by a mean circular flow $\omega(r)$ with shear $S(r)$.

The Hamiltonian describing this dynamics is

$$H=\int_0^{r_a} r\,dr\,\gamma_a\omega(r)+\int_0^{r_b} r\,dr\,\gamma_b\omega(r) + \frac{\gamma_a\gamma_b}{4\pi}\ln[|\mathbf{r}_a-\mathbf{r}_b|^2], \tag{3}$$

with equations of motion

$$\frac{d\theta_a}{dt}=\frac{\partial H}{\partial P_{\theta_a}}, \quad \frac{dP_{\theta_a}}{dt}=-\frac{\partial H}{\partial \theta_a} \tag{4}$$

(and similarly for vortex b), where $P_{\theta_a}=\gamma_a r_a^2/2$ is the canonical angular momentum associated with vortex a and (r_a,θ_a) are polar coordinates. The symmetry of H under rotation implies that total angular momentum is conserved: $P_{\theta_a}+P_{\theta_b}=$ constant. Let us define this constant in terms of a mean radial position R for the two vortices:

$$P_{\theta_a}+P_{\theta_b}=(\gamma_a+\gamma_b)R^2/2. \tag{5}$$

Then assuming that vortices are closely spaced so that $|\mathbf{r}_a-\mathbf{r}_b|/R\ll 1$, it is useful to work in a frame rotating with frequency $\omega(R)$, where the Hamiltonian is transformed to

$$H'=H-(P_{\theta_a}+P_{\theta_b})\omega(R). \tag{6}$$

Defining $\Delta r_{a,b}=r_{a,b}-R$, we Taylor expand H' to second order in $\Delta r_{ab}/R$ and $\theta_a-\theta_b$. The result is

$$H'=\frac{S}{2}(\gamma_a\Delta r_a^2+\gamma_b\Delta r_b^2)+\frac{\gamma_a\gamma_b}{4\pi}\ln[(r_a-r_b)^2 + R^2(\theta_a-\theta_b)^2], \tag{7}$$

where $S=S(R)$. The equations of motion that follow from Eq. (7) are

$$\frac{dr_a}{dt}=-\frac{\gamma_b R}{2\pi}\frac{\theta_a-\theta_b}{(r_a-r_b)^2+R^2(\theta_a-\theta_b)^2}, \tag{8a}$$

$$R\frac{d\theta_a}{dt}=S\Delta r_a+\frac{\gamma_b}{2\pi}\frac{r_a-r_b}{(r_a-r_b)^2+R^2(\theta_a-\theta_b)^2}, \tag{8b}$$

and similarly for vortex b. Equation (8a) implies that $\gamma_a r_a+\gamma_b r_b=$ const. To first order in $\Delta r_{ab}/R$ this is equivalent to Eq. (5), and this equation allows us to identify the constant as $\gamma_a r_a+\gamma_b r_b=(\gamma_a+\gamma_b)R$. However, this implies that

$$\gamma_a\Delta r_a+\gamma_b\Delta r_b=0. \tag{9}$$

Furthermore, Eqs. (8b) and (9) imply that $\gamma_a\theta_a+\gamma_b\theta_b=$ const. If we define $\Theta=(\gamma_a\theta_a+\gamma_b\theta_b)/(\gamma_a+\gamma_b)$, we can then see that the position of the ''center of charge'' $\mathbf{R}\equiv(R,\Theta)$ is conserved in the dynamics (to first order in $\theta_a-\theta_b$ and $\Delta r_{a,b}/R$); in other words, the displacements $\Delta\mathbf{r}_{a,b}=\mathbf{r}_{a,b}-\mathbf{R}\equiv(\Delta r_{a,b},\,\Delta\theta_{a,b})$ satisfy

$$\gamma_a\Delta\mathbf{r}_a+\gamma_b\Delta\mathbf{r}_b=\mathbf{0}. \tag{10}$$

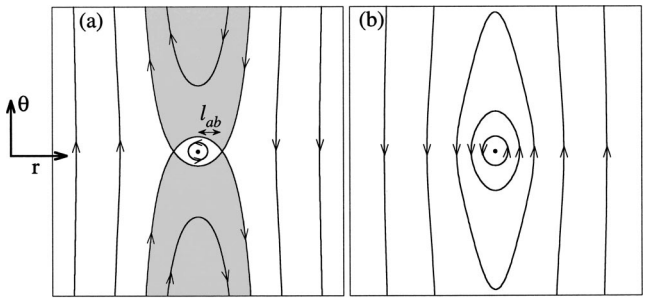

FIG. 1. Flow diagram for (a) retrograde flow $S(\gamma_a+\gamma_b)<0$; (b) prograde flow $S(\gamma_a+\gamma_b)>0$.

If we now use this relationship between the vortex positions in Eq. (7), we can write the Hamiltonian in terms of only the position of vortex a:

$$H'(r_a,\theta_a)=\frac{S}{2}\frac{\gamma_a(\gamma_a+\gamma_b)}{\gamma_b}\Delta r_a^2+\gamma_a\gamma_b 4\pi \times\ln\left[\left(1+\frac{\gamma_a}{\gamma_b}\right)^2(\Delta r_a^2+R^2\Delta\theta_a^2)\right]. \tag{11}$$

The contours of constant H' are shown in Fig. 1, blowing up a region centered on $\mathbf{r}=\mathbf{R}$, and with $\mathbf{R}$ assumed to be on the positive x axis, i.e., $\Theta=0$, so $\Delta\theta_a=\theta_a$. Thus, the center of the circular flow, $r=0$, is well to the left of the figure, and the x direction corresponds to r, while the y direction corresponds to θ. In Fig. 1(a), the H' contours are drawn assuming $S(\gamma_a+\gamma_b)<0$. This is termed a ''retrograde flow.'' The opposite case, $S(\gamma_a+\gamma_b)>0$, is shown in Fig. 1(b), and is termed a ''prograde flow.'' In these diagrams, vortex a follows one of the constant-H contours shown, and the b vortex is at the point

$$\Delta\mathbf{r}_b=-\gamma_a\Delta\mathbf{r}_a/\gamma_b, \tag{12}$$

according to Eq. (10).

For the case of retrograde flow, a separatrix in the flow exists, with X points for vortex a at locations $(\Delta r_a,\theta_a)=(\pm l_{ab},0)$ where the trapping width l_{ab} is defined as

$$l_{ab}=\sqrt{-2\gamma_b^2/[4\pi(\gamma_a+\gamma_b)S]}. \tag{13}$$

The equation for the separatrix, $\Delta r_s(\theta)$, of vortex a is

$$\Delta r_s^2=l_{ab}^2(1+\ln[(\Delta r_s^2+R^2\theta^2)/l_{ab}^2]). \tag{14}$$

The b vortex separatrix has the same form, but is scaled by the factor γ_a/γ_b. Vortices located on streamlines outside their respective separatrices stream past one another, and do not suffer any net change in their x positions from their interaction. However, vortices within the separatrix region [the shaded region in Fig. 1(a)] reflect off of one another, and therefore take a step in the r direction due to their collision.

For the remainder of the paper, we focus exclusively on retrograde flow, $S(\gamma_a+\gamma_b)<0$. The case of prograde flow was examined numerically in Ref. 9. No theory has yet been developed that covers this case. We will briefly return to the prograde case in Sec. IV.

For retrograde flow, we use the previous picture of a two-body collision to determine the test-particle diffusion coefficient for diffusion of vortex a in the r direction due to collisions with vortices of type b. Vortex a encounters a sequence of randomly distributed vortices of type b moving past it. The flux of b vortices in the θ direction, $\Gamma_{\theta b}$, is determined by the shear, as

$$\Gamma_{\theta b}=n_b S\Delta\rho. \tag{15}$$

Here, n_b is the areal density (in cm^{-2}) of the b vortices, and $\Delta\rho=\Delta r_b-\Delta r_a$ is the r displacement (impact parameter) between the a and b vortices when the vortices have a large θ displacement (i.e., before this collision begins, but after the previous collision with some other vortex has ended). Let us call this θ-distance θ_0. Then it is not difficult to show that if $\Delta\rho$ satisfies

$$|\Delta\rho|\leqslant|(\gamma_a+\gamma_b)/\gamma_b|\Delta r_s(\theta_0), \tag{16}$$

vortex a will be within its separatrix and take a step in the x direction of magnitude $|2\gamma_b\Delta\rho/(\gamma_a+\gamma_b)|$.

The test particle diffusion coefficient D_{ab}^B due to these Boltzmann collisions between vortices of type a and b is given by half the square of this step, multiplied by the rate at which these steps occur, and integrated over all impact parameters that lead to a finite step. This can be written

$$D_{ab}^B=\frac{1}{2}\int_{-(\gamma_a+\gamma_b)\Delta r_s(\theta_0)/\gamma_b}^{(\gamma_a+\gamma_b)\Delta r_s(\theta_0)/\gamma_b}d\Delta\rho\left(\frac{2\gamma_b}{\gamma_a+\gamma_b}\Delta\rho\right)^2|\Gamma_{\theta b}| =n_b|S|[(\gamma_a+\gamma_b)/\gamma_b]^2\Delta r_s^4(\theta_0), \tag{17}$$

where in the second line we have used Eq. (15). Since $R\theta_0\gg l_{ab}$, the solution of Eq. (14) for $\Delta r_s(\theta_0)$ is

$$\Delta r_s(\theta_0)\approx l_{ab}\sqrt{\ln(R^2\theta_0^2/l_{ab}^2)}. \tag{18}$$

Using Eq. (13) for l_{ab} then yields

$$D_{ab}^B=\frac{\gamma_b^2 n_b}{4\pi^2|S|}\ln^2[R^2\theta_0^2/l_{ab}^2]. \tag{19}$$

This expression generalizes our previous single-species result[9] to multiple vortex species. The diffusion scales as $1/|S|$, displaying the same shear reduction of transport obtained previously for one species.

The argument of the logarithm depends on θ_0, the mean θ displacement (mean-free path) between collisions. We can estimate this displacement as follows. The cross section for collisions between a species b vortex and species a is roughly $2|(\gamma_a+\gamma_b)l_{ab}/\gamma_b|$ [see Eqs. (16) and (14)], so the mean free path for b vortices is

$$R\theta_0\approx\left|\frac{\gamma_b}{2\Sigma_a(\gamma_a+\gamma_b)l_{ab}n_a}\right| =\left(\sum_a n_a\sqrt{-2(\gamma_a+\gamma_b)/\pi S}\right)^{-1}, \tag{20}$$

where the sum is over all species a. Equation (19) is valid provided that collisional events are well separated in space and time, that is, $R\theta_0>l_{ab}$.

III. KUBO ANALYSIS OF DISTANT COLLISIONS

A. Radial diffusion

Equation (19) neglects the diffusive effect of collisions with large impact parameters. In the two-particle Boltzmann picture, such collisions produce no net radial step because the vortex deflection in the first half of the collision is exactly reversed in the second half. However, these large impact parameter collisions are not isolated events, and interactions with the surrounding vortices break the time symmetry of the idealized two-body collision.

First we determine the radial diffusion caused by multiple large impact parameter collisions. To do so, we focus on a specific ''test'' vortex, located at position $\mathbf{r}(t)$. This vortex feels a fluctuating velocity field $\delta\mathbf{v}(r,t)$, due to the cumulative effect of interactions with many distant vortices. The fluctuation can be written as a sum of pairwise interactions,

$$\delta\mathbf{v}(r,t)=-\sum_{p=1}^{N}\frac{\partial\phi_p}{\partial\mathbf{r}}(|\mathbf{r}-\mathbf{r}_p|)\times\hat{z}, \tag{21}$$

where the sum runs over the N vortices in the system, at positions $\mathbf{r}_p(t)$, and $\phi_p(|\mathbf{r}-\mathbf{r}_p|)=(\gamma_p)/(4\pi)\ln[|\mathbf{r}-\mathbf{r}_p|]$ is the stream function created by the pth vortex at the test vortex location $\mathbf{r}(t)$.

The radial component of this velocity fluctuation causes radial diffusion of the test vortex according to the Kubo formula

$$D^K=\int_0^\infty dt\langle\delta v_r(t)\,\delta v_r(0)\rangle, \tag{22}$$

where the $\langle\cdot\rangle$ indicates an average over an ensemble of identically prepared systems. The ensemble average and time integral can be easily evaluated using standard kinetic theory techniques. First, the radial velocity fluctuation is decomposed into azimuthal Fourier modes:

$$\delta v_r(t)=\sum_{p=1}^{N}\frac{\gamma_p}{4\pi r}\sum_{\substack{m=-\infty\\ m\neq 0}}^{\infty}\frac{im}{|m|}e^{im(\theta-\theta_p)}\left(\frac{r_<}{r_>}\right)^{|m|}, \tag{23}$$

where $r_{<(>)}$ is the lesser (greater) of r and r_p. Next, the trajectory of each vortex is specified using the approximation of integration along unperturbed orbits: each of the $p=1,\ldots,N$ vortices rotate about the center of the overall vortex patch, with

$$\begin{aligned} r_p&=r_{p_0},\\ \theta_p(t)&=\omega(r_p)t+\theta_{p_0}. \end{aligned} \tag{24a}$$

Similarly the trajectory of the test vortex is given by

$$\begin{aligned} r&=r_0,\\ \theta(t)&=\omega(r)t+\theta_0. \end{aligned} \tag{24b}$$

The ensemble average is then evaluated using standard techniques for random distributions, converting $\langle\Sigma_p\Sigma_{\bar{p}}\gamma_p\gamma_{\bar{p}}\cdots\rangle$ to $\Sigma_{\bar{p}}\delta p\bar{p}\int r_p\,dr_p\,d\theta_{p_0}\Sigma_b\gamma_b^2 n_b(r_p)\cdots$, where n_b is the density of vortices of type b.

Substituting these results into Eq. (22) yields an expression for the radial diffusion coefficient,

$$\begin{aligned} D^K=\sum_b\frac{\gamma_b^2}{(4\pi r)^2}&\sum_{\substack{m=-\infty\\ m\neq 0}}^{\infty}\sum_{\substack{\bar{m}=-\infty\\ \bar{m}\neq 0}}^{\infty}\frac{(-)m\bar{m}}{|m||\bar{m}|}\\ &\times\int_0^\infty dt\int_0^\infty r_p\,dr_p\int_0^{2\pi}d\theta_{p_0}\,n_b(r_p)\\ &\times e^{i(m+\bar{m})(\theta_0-\theta_{p_0})+im[\omega(r)-\omega(r_p)]t}\left(\frac{r_<}{r_>}\right)^{|m|+|\bar{m}|}. \end{aligned} \tag{25}$$

Evolution of the t and θ_{p_0} integrals implies that only the $\bar{m}=-m$ term contributes, giving

$$\begin{aligned} D^K=\sum_b\frac{\gamma_b^2}{(4\pi r)^2}&\sum_{\substack{m=-\infty\\ m\neq 0}}^{\infty}2\pi^2\int_0^\infty r_p\,dr_p\,n_b(r_p)\\ &\times\delta(m[\omega(r)-\omega(r_p)])\left(\frac{r_<}{r_>}\right)^{2|m|}. \end{aligned} \tag{26}$$

The δ function can then be evaluated, yielding

$$D^K=\sum_b\frac{\gamma_b^2 n_b(r)}{8|S|}\sum_{\substack{m=-\infty\\ m\neq 0}}^{\infty}\frac{1}{|m|}. \tag{27}$$

Here, we have dropped contributions (if any) to the radial integral from points that satisfy $\omega(r_p)=\omega(r)$ with $r_p\neq r$, which can occur for nonmonotonic rotation frequency profiles.[12]

These contributions to D^K are, typically, smaller than the $r=r_p$ term because the sum over m in Eq. (26) converges when $r_p\neq r$.

For $r_p=r$, however, the sum is logarithmically divergent at large m. This divergence occurs because nearby vortices following unperturbed orbits take a long time to separate, and therefore take a large radial step. The sum can be cut off by noting that there is a minimum separation d for which unperturbed orbits are a good approximation. Adding the cutoff to Eq. (27) implies

$$D^K=\sum_b D^K_{ab}, \tag{28}$$

where

$$D^K_{ab}=\frac{\gamma_b^2 n_b(r)}{4|S(r)|}\ln\left(\frac{r}{d}\right) \tag{29}$$

is the diffusion coefficient of species a due to long-range collisions with species b.

One possible estimate for the minimum separation d is the trapping distance l_{ab}, since vortices separated by l_{ab} do not follow unperturbed orbits. Another possibility is that vortices diffuse apart before they are carried away by the shear, and so cannot be treated with unperturbed orbit theory. For vortices separated in r by a distance δ, the time to shear apart a distance of order δ is given by $1/|S|$, and the time to diffusively separate by a distance δ is $\delta^2/4D^K$. Equating the two times gives the diffusion-limited minimum separation $\delta=[4D^K/|S|]^{1/2}$. With these two processes degrading small impact parameter collisions, the best estimate for d in Eq. (29) is

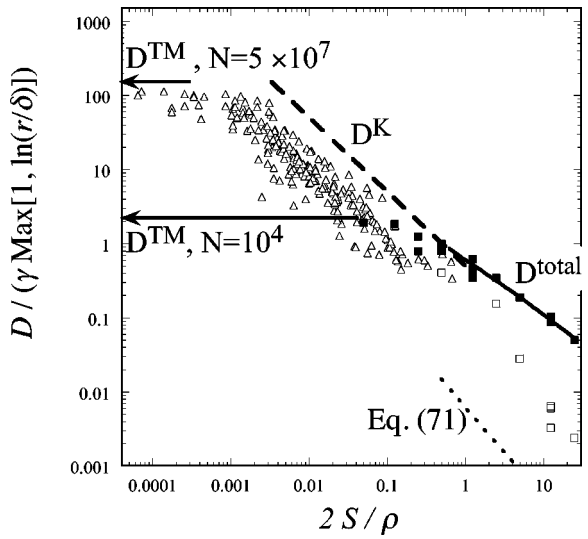

FIG. 2. Diffusion versus shear rate in a single species point vortex gas. Solid and open squares are simulation results for retrograde and prograde flows, respectively (Ref. 9). Open triangles are results of experiments on pure ion plasmas (Ref. 19). Solid line, Eq. (31) for total D_{aa} assuming $N=10\,000$ identical vortices, in a circular patch of uniform vorticity (as in the simulations). Dashed line, Eq. (29) for D_{aa}^K, taking $d=\delta$. Dotted line, Eq. (71).

$$d=\mathrm{Max}(\delta,l_{ab}). \tag{30}$$

For the case where $\delta>l_{ab}$, this somewhat *ad hoc* approach to the logarithmic divergence can be put on firmer footing by keeping the effect of fluctuations in the vortex trajectories. This will be discussed in Appendix A.

Finally, the total radial diffusion coefficient from small and large impact parameter collisions is the sum of the Boltzmann and Kubo analyses,

$$D_{ab}^{\mathrm{total}}=D_{ab}^B+D_{ab}^K. \tag{31}$$

Equation (31) is correct only when the shear is large enough so that $D^{\mathrm{total}}<D^{\mathrm{TM}}$, where D^{TM} is the zero-shear result given by Eq. (2). However, comparing Eqs. (2) and (31), we see that only a small shear, $S/\rho\sim O(1/N^{1/2})$, is required to meet this inequality. In other words, small shears wipe out the large-scale Dawson–Okuda vortices responsible for the diffusion predicted by Eq. (2).

Figure 2 summarizes the theory and compares it to recent simulations and experiments. The theoretical prediction (solid line) for D_{aa}^{total} is plotted versus a normalized shear rate $2S/\rho$. Computer simulations of diffusion in retrograde flows consisting of $N=10^4$ identical point vortices are shown as solid squares, and can be seen to match the theory well,[9] provided that the shear is sufficiently large. For small shears the simulations approach the Taylor–McNamara result[2] for 10^4 vortices, shown by the lower arrow on the left.

Also shown in the same figure are experimental results for diffusion, measured recently in a pure ion plasma experiment (open triangles).[19] The number of charges in the plasma was $N=5\times10^7$. For very low shears, the experimental diffusion again approaches the Taylor–McNamara result (the upper arrow on the left) which is larger than in the simulations because of the larger number of particles in the experiment: see Eq. (2). For larger shear, we compare the experiment to the Kubo diffusion D_{aa}^K (dashed line) since the density is too high for Boltzmann collisions to enter. The trend in the experimental data matches the Kubo theory with no adjustable parameters, although the absolute magnitude is off by roughly a factor of 4. The reason for this discrepancy is unknown, but could be due either to the difficulty of measuring small shears in the experiments, or to the fact that the plasma is not well into the 2D regime. For data shown in the range $2S/\rho\gtrsim0.1$ the bounce frequency of the ions along the magnetic field is smaller than the shear rate, indicating that the plasma ions cannot be well approximated by bounce-averaged rods of charge. Clearly, more work needs to be done before we can say that the theory explains the experiments in detail. Nevertheless, it is apparent that the shear reduction of the diffusive transport is well represented by the theory, for retrograde flow.

However, for prograde flows, the theory fails. Diffusion measured in simulations of prograde flow (open squares) shows a different dependence on shear rate than the theory, and is up to an order of magnitude smaller than the prediction of Eq. (31). We will return to the issue of diffusion in prograde flow in Sec. IV.

B. Azimuthal diffusion and superdiffusion

So far we have focused on diffusion in the radial direction because this is what can be most easily observed in experiments. However, the velocity fluctuations given by Eq. (21) imply that diffusion occurs in the θ direction as well. The Kubo expression for diffusion in the θ direction is

$$D_\theta^K=\int_0^\infty dt\langle\delta v_\theta(t)\,\delta v_\theta(0)\rangle. \tag{32}$$

This diffusion coefficient can be evaluated in an analogous manner to the previous derivation of radial diffusion. The result analogous to Eq. (26) is

$$D_\theta^K=\sum_b\frac{\gamma_b^2}{(4\pi)^2}\sum_{\substack{m=-\infty\\ m\neq0}}^{\infty}\frac{2\pi^2}{m^2}\int_0^\infty r_p\,dr_p\,n_b(r_p)\times\delta(m[\omega(r)-\omega(r_p)])\left[\frac{\partial}{\partial r}\left(\frac{r_<}{r_>}\right)^{|m|}\right]^2. \tag{33}$$

Taking the derivative and then evaluating the δ function (again keeping only the contribution from $r_p=r$) yields

$$D_\theta^K=\sum_b\frac{\gamma_b^2 n_b(r)}{8|S|}\sum_{\substack{m\neq0\\ m=\infty}}^{\infty}\frac{1}{|m|} \tag{34}$$

which is identical to Eq. (27). This implies that the diffusion coefficient from large impact parameter collisions is isotropic, even in the presence of shear, i.e., $D_\theta^K=D^K$. However, this Kubo expression for diffusion does not provide a complete picture of the θ dynamics in the sheared flow.

We now use an analysis based on the Langevin equation to show that the θ dynamics is superdiffusive. Consider a test vortex located initially at position $(r_0,\ \theta_0)$. Then in a frame rotating with the local rotation frequency $\omega(r_0)$, a Langevin picture of the dynamics leads to the equations of motion

$$\frac{dr}{dt}=\delta v_r(t),$$
$$r\frac{d\theta}{dt}=\omega(r)-\omega(r_0)+\delta v_\theta(t), \tag{35}$$

where δv_r and δv_θ are the fluctuating velocity fields given by Eq. (21). If we linearize these equations with respect to the radial excursion $\delta r(t)$, and define $\delta\theta=\theta-St-\theta_0$, we obtain

$$\frac{d\delta r}{dt}=\delta v_r(t),$$
$$r_0\frac{d\delta\theta}{dt}=S\,\delta r+\delta v_\theta(t), \tag{36}$$

where $S=r_0\,d\omega/dr_0$ is the shear rate. A standard Langevin analysis of these equations then yields for the radial diffusion

$$\langle\delta r^2(t)\rangle=2\int_0^t dt'\langle\delta v_r(t')\delta v_r(0)\rangle(t-t'). \tag{37}$$

For times long compared to the autocorrelation time τ, defined as

$$\tau=\int_0^\infty dt'\,t'\langle\delta v_r(t')\delta v_r(0)\rangle/D^K, \tag{38}$$

Eq. (37) yields the usual result for diffusion in one (radial) dimension:

$$\langle\delta r^2(t)\rangle=2D^K(t-\tau),\quad t\gg\tau \tag{39}$$

with D^K given by Eq. (22).

However, for the θ dynamics, the same analysis implies

$$r_0^2\langle\delta\theta^2(t)\rangle=\tfrac{2}{3}S^2D^Kt^3+2D_\theta^Kt,\quad t\gg\tau, \tag{40}$$

where we have neglected terms involving the autocorrelation time τ. Thus, the θ dynamics is superdiffusive, scaling as t^3 for large t. Note that Eq. (38) implies the autocorrelation time is of order S^{-1}, and since $D_\theta^K=D^K$, we can therefore drop the second term in Eq. (40) to the order of approximation we are working. The origin of the superdiffusion is clear: as particles diffuse radially, they are swept away in θ by the shear flow at a rate which is more rapid than their rate of diffusion in θ.

The shear also creates a correlation between θ and r dynamics,

$$r_0\langle\delta\theta(t)\delta r(t)\rangle=SD^Kt^2,\quad t\gg\tau. \tag{41}$$

This correlation of $\delta\theta$ with δr is easy to understand: as a vortex takes a positive step δr, it moves into a shear flow that tends to increase $\delta\theta$ for $S>0$ and decrease $\delta\theta$ for $S<0$. These correlations are similar in form to those which occur between velocity and position at early times in Brownian motion. Furthermore, although Eq. (40) keeps only the diffusive effects of large-impact-parameter collisions, we expect that Boltzmann collisions treated in Sec. II would produce the same effects, so that we should replace D^K by D^{total} in Eq. (40).

C. Klimontovitch approach to radial diffusion

It is instructive to derive the radial diffusion due to large-impact-parameter collisions using a different approach, based on the Klimontovitch formalism. In this approach the diffusive flux is derived by suitable averaging of the Klimontovitch equation for a system of N point vortices.

Each species of vortex, with circulation γ_a, is described by a separate Klimontovitch vorticity $\eta_a(\mathbf{r},t)$, where

$$\eta_a(\mathbf{r},t)=\sum_{p=1}^{N_a}\gamma_a\delta(\mathbf{r}-\mathbf{r}_p(t)) \tag{42}$$

and N_a is the number of vortices of type a. The mean vorticity of species a is $\zeta_a(\mathbf{r},t)=\langle\eta_a\rangle$, where the average is over an ensemble of macroscopically identical systems. The Klimontovitch vorticity satisfies the Klimontovitch equation

$$\frac{\partial\eta_a}{\partial t}-\nabla\Psi\times\hat{z}\cdot\nabla\eta_a=0, \tag{43}$$

where $\Psi(\mathbf{r},t)$ is the stream function of the system, which satisfies the Poisson equation

$$\nabla^2\Psi(\mathbf{r},t)=\sum_a\eta_a(\mathbf{r},t). \tag{44}$$

In order to derive a diffusive radial flux from Eqs. (42)–(44), one assumes that the mean vorticity for each species is a function only of radius:

$$\zeta_a=\zeta_a(r,t). \tag{45}$$

The mean stream function $\psi(r,t)\equiv\langle\Psi(\mathbf{r},t)\rangle$ is then also cylindrically symmetric according to the average of Eq. (44). Fluctuations away from the mean are described by $\delta\zeta_a(\mathbf{r},t)\equiv\eta_a(\mathbf{r},t)-\zeta_a(r,t)$ and $\delta\psi(\mathbf{r},t)\equiv\Psi(\mathbf{r},t)-\psi(r,t)$. By averaging Eq. (43), the radial flux J_{r_a} of vorticity arising from species a can be written in terms of these fluctuations:

$$\frac{\partial\zeta_a}{\partial t}+\frac{1}{r}\frac{\partial}{\partial r}(rJ_{r_a})=0, \tag{46}$$

where

$$J_{r_a}=-\left\langle\frac{1}{r}\frac{\partial\delta\psi}{\partial\theta}\delta\zeta_a\right\rangle. \tag{47}$$

The vorticity flux J_{r_a} is related to the particle flux Γ_{r_a} by $\Gamma_{r_a}=J_{r_a}/\gamma_a$. (The vorticity flux is equivalent to radial current density in the plasma analogue of this system.) The fluctuations can be evaluated approximately by linearizing Eqs. (43) and (44),

$$\frac{\partial\delta\zeta_a}{\partial t}+\omega\frac{\partial\delta\zeta_a}{\partial\theta}-\frac{1}{r}\frac{\partial\delta\psi}{\partial\theta}\frac{\partial\zeta_a}{\partial r}=0, \tag{48}$$

$$\nabla^2\delta\psi=\sum_a\delta\zeta_a, \tag{49}$$

where $\omega=\omega(r,t)=r^{-1}\partial\psi(r,t)/\partial r$ is the mean rotation frequency.

The solution of Eqs. (48) and (49) is most easily expressed by Fourier and Laplace transformation of $\delta\zeta$ and $\delta\psi$

in θ and t, respectively, under the assumption that fluctuations evolve rapidly compared to the transport time scale, so that time variation of ω and ζ_a can be neglected; this is the Boguliubov ansatz. The transformed stream function $\delta\hat{\psi}$ is defined by

$$\delta\psi(r,\theta,t)=\sum_{m=-\infty}^{\infty} e^{im\theta}\int \frac{ds}{2\pi i}e^{st}\delta\hat{\psi}(r,m,s), \tag{50}$$

with a similar definition for $\delta\hat{\zeta}_a(r,m,s)$. The solutions of Eqs. (48) and (49) for $\delta\hat{\psi}$ are then given by a Green's function,

$$\delta\hat{\psi}=-\sum_a \sum_{p=1}^{N_a} \frac{\gamma_a}{2\pi}\frac{e^{-im\theta_{p_0}}}{s+il\omega(r_p)}G(r,r_p,m,s). \tag{51}$$

The Green's function G satisfies

$$\left[\frac{1}{r}\frac{\partial}{\partial r}r\frac{\partial}{\partial r}-\frac{m^2}{r^2}+\sum_a \frac{im}{s+im\omega(r)}\frac{\partial\zeta_a}{\partial r}\right]G(r,r_p,m,s) = \frac{\delta(r-r_p)}{r}, \tag{52}$$

where θ_{p_0} is the initial θ location of vortex p, and r_p is its radial location. The solution for $\delta\hat{\zeta}_a$ in terms of $\delta\hat{\psi}$ is then

$$\delta\hat{\zeta}_a=\frac{im\delta\hat{\phi}\frac{\partial\zeta_a}{\partial r}+\sum_{p=1}^{N_a}\gamma_a\delta(r-r_p)e^{im\theta_{p_0}}/2\pi}{r(s+im\omega(r))}. \tag{53}$$

The vorticity flux of species a is obtained from Eqs. (51)–(53), with the assumption of random statistics for the initial vortex positions:

$$J_{r_a}(r)=-\frac{1}{2r}\sum_m |m|\int r_p\,dr_p|G(r,r_p,m,-im\omega(r))|^2 \times\delta[\omega(r)-\omega(r_p)]\sum_b\left(\frac{\gamma_b\zeta_b(r_p)}{r}\frac{\partial\zeta_a(r)}{\partial r} -\frac{\gamma_a\zeta_a(r)}{r_p}\frac{\partial\zeta_b(r_p)}{\partial r_p}\right). \tag{54}$$

Details of the algebra leading to Eq. (54) can be found in Ref. 12 for the case of a single species; and the addition of multiple species to the problem is straightforward.

To obtain an expression for diffusive flux from Eq. (54), we evaluate the radial integral assuming that the dominant contribution from the δ function occurs at $r_p=r$, just as in Sec. III A. The flux can be then written in terms of local diffusion coefficients, as

$$J_{r_a}=-\sum_b\left[D_{ab}^K\frac{\partial\zeta_a}{\partial r}-\overline{D}_{ab}^K\frac{\partial\zeta_b}{\partial r}\right], \tag{55}$$

where

$$D_{ab}^K=\frac{\gamma_b\zeta_b}{2|S|}\sum_{\substack{m=-\infty\\ m\neq 0}}^{\infty}|m||G(r,r,m,-im\omega(r))|^2 \tag{56}$$

is the diffusion coefficient for species a due to collisions with species b, and $\overline{D}_{ab}^K$ is an "off-diagonal" diffusion coefficient related to D_{ab}^K through the equation

$$\overline{D}_{ab}^K=\frac{\gamma_a\zeta_a D_{ab}^K}{\gamma_b\zeta_b}. \tag{57}$$

These off-diagonal terms are commonly found in multispecies systems,[20] but cannot be derived from the Kubo approach of Sec. III A. Equation (56) is a generalization of Eq. (27) that allows for the influence of collective effects on the interaction between vortices. When collective effects are neglected, one drops the term proportional to $\partial\zeta_a/\partial r$ in Eq. (52), resulting in a bare Green's function

$$G^{\text{bare}}(r,r,m,-im\omega(r))=-\frac{1}{2|m|}.$$

Substituting this into Eq. (56) returns us to Eq. (27), showing the quasilinear Kubo calculation of Sec. III A agrees with the Klimontovitch analysis. Furthermore, we have already seen in Sec. III A that the diffusion coefficient is dominated by high azimuthal mode numbers, where the bare-interaction approximation is valid.

A similar expression for D_{aa}^K in a single-species system has been derived by Chavanis,[16] although that author does not address the form of the cutoff to the logarithmic divergence. However, his flux equation, Eq. (28) of Ref. 16, is incorrect, yielding a nonzero diffusive flux when only a single species is present. Flux equations for multiple species systems involving mobility flux have also been put forward by other authors,[17] but these also incorrectly yield a nonzero diffusion flux for a single-species system. For a single species, we see that $\overline{D}_{aa}^K=D_{aa}^K$, and Eq. (55) correctly yields zero diffusion flux. It is well known that momentum conservation requires that the dissipative flux must be viscous, not diffusive, when there is only a single species.[21]

Equations (56) and (57) imply that the off-diagonal diffusion terms $\overline{D}^K$ satisfy the expected Onsager relation for a point vortex gas,

$$\frac{\overline{D}_{ab}}{\gamma_a\zeta_a}=\frac{\overline{D}_{ba}}{\gamma_b\zeta_b}, \tag{58}$$

as shown in Appendix B. These off-diagonal terms create a flux of species a up or down a gradient in the vorticity from species b. This flux is equivalent to the drift of vortices up and down a background vorticity gradient, analyzed in Ref. 13. The radial drift velocity $v_{r_a}=J_{r_a}/\zeta_a$ is given by

$$v_{r_a}=-\frac{\overline{D}_{ab}^K}{\zeta_a}\frac{\partial}{\partial r}\zeta_b(r). \tag{59}$$

An identical expression was derived in Ref. 13 using different methods and was found to work well in describing the motion of individual retrograde vortices up or down a gradient in the background vorticity, provided that the correct logarithmic cutoff is introduced. For the case of Ref. 13, species a vortices had very large circulation compared to species b (the background vortices), and the cutoff d in Eq. (29) is then given by l_{ab}.

D. Diffusive plasma dynamics

Before we continue with a discussion of the test-particle diffusion coefficient itself, it is useful to consider some of the plasma dynamics that follows from the particle flux equations, Eq. (55). The conservation properties of the equations are relatively straightforward and of sufficient importance to merit discussion here. First, one can easily show that Eqs. (55), (57), and (58) imply

$$\sum_a J_{r_a} = 0, \tag{60}$$

i.e., the total radial current is zero. This is dictated by conservation of canonical angular momentum in a binary collision, together with the fact that when two particles make a collisional step, they are at the same radius due to the resonance condition (δ function) in Eq. (54).

Equation (60) implies that the total vorticity profile $\rho(r)$ does not change with time in the evolution:

$$\sum_a \zeta_a(r,t) = \rho(r). \tag{61}$$

The vorticity of individual species may rearrange, but total vorticity $\rho(r)$ is a fixed function of position, determined by the initial condition. From this it follows trivially that total canonical angular momentum density and potential energy density are constant in time. Under these dynamics, the system cannot approach a state of thermal equilibrium (where the rotation frequency is radially uniform) from an arbitrary initial condition; to do so would require viscous fluxes that are not included in Eqs. (55).

Nevertheless, one can show that there is an H theorem, and that dissipation leads to separation and concentration of each species, with no change in total vorticity. For the entropy functional

$$\mathcal{S}(t) = -\sum_a \int d^2r \frac{\zeta_a(r,t)}{\gamma_a} \ln \zeta_a(r,t), \tag{62}$$

a few lines of algebra show that $d\mathcal{S}/dt \geqslant 0$ (see Appendix C). The increase of entropy is due to a dissipative rearrangement of the vorticity of each species; species with higher circulation γ_a tend to concentrate in regions of higher total vorticity. This can be proven as follows. The equilibrium state is one for which $J_{r_a} = 0$. Equations (55) and (57) then imply the following equilibrium relation between the densities:

$$\zeta_b(r) = C_b[\zeta_a(r)]^{\gamma_b/\gamma_a}, \tag{63}$$

where C_b is a constant. Equation (63) implies a Boltzmann-type form for the equilibrium vorticity of each species, $\zeta_b(r) = \zeta_{b_0} \exp[-\gamma_b \chi(r)/T]$ where ζ_{b_0} and T are constants, and $\chi(r)$ is a function determined by the initial conditions (i.e., the total circulation in each species, and the total vorticity as a function of radius). However, identification of the function $\chi(r)$ with the stream function $\psi(r)$ is possible only provided that the plasma is in a state of overall thermal equilibrium, where overall fluid rotation frequency $\omega(r)$ is independent of r.

Assume for simplicity that there are only two species, a and b, and that $\gamma_a > 0$. Equations (61) and (63) then become

$$C_b \zeta_a^{\gamma_b/\gamma_a} + \zeta_a = \rho. \tag{64}$$

Two cases must be examined: (i) $\gamma_b > \gamma_a$ and (ii) $\gamma_b < 0$. The case $0 < \gamma_b < \gamma_a$ can be obtained from case (i) by flipping species labels. For case (i), Eq. (63) implies that $C_b > 0$, so the left-hand side of Eq. (64) is a monotonically increasing function of ζ_a.

Therefore, ζ_a is a monotonically increasing function of ρ. However, Eq. (63) also implies

$$\frac{\zeta_b}{\zeta_a} = C_b \zeta_a^{(\gamma_b/\gamma_a)-1}. \tag{65}$$

Thus, if $\gamma_b > \gamma_a$, ζ_b/ζ_a is a monotonically increasing function of ζ_a, which monotonically increases with ρ. Therefore ζ_b/ζ_a increases as ρ increases, proving that species b, with $\gamma_b > \gamma_a$, concentrates at larger ρ.

For case (ii), we must have $C_b < 0$ in Eqs. (64) and (65). One can then easily see that ζ_a is still monotonically increasing in ρ, but that $|\zeta_b/\zeta_a|$ monotonically decreases in ρ. Thus, our conclusion remains unchanged: species a, with $\gamma_a > \gamma_b$, concentrates at larger ρ.

Concentration of vortices with large circulation around peaks of the vorticity may seem counterintuitive in a diffusive process. However, it can be thought of as an extension to many vortices of the motion of a positive (or negative) single vortex up (or down) a background vorticity gradient, well-known to fluids researchers.[13,14] It has been suggested that such motion could lead to the formation of zonal flows,[22] by amplifying vorticity peaks as new vortices move toward them. Unfortunately, our analysis shows that diffusive vortex dynamics leaves the overall flow field unchanged, so zonal flows do not develop from the fluxes described by Eq. (55).

The equilibrium predicted by Eq. (63) can be easily observed in simulations. Below we show the results of a molecular dynamics simulation of $N = 2000$ point vortices, consisting of two species: $N_1 = 1000$ of species 1 with circulation $\gamma_1 = \gamma$, and $N_2 = 1000$ of species 2 with circulation $\gamma_2 = \gamma/2$. The density of each species is initially chosen to be the same:

$$\begin{aligned} n_1(r,0) = n_2(r,0) &= \frac{3N}{2\pi R^2}\left(1 - \frac{r}{R}\right), \\ & r < R = 0, \quad r > R, \\ \rho(r,0) &= \frac{9N\gamma}{4\pi R^2}\left(1 - \frac{r}{R}\right), \quad r < R. \end{aligned} \tag{66}$$

Over time, we observe that the density of species 1 concentrates near the center compared to that of species 2. The evolution of mean square radius $\langle r^2 \rangle_i(t)$ for each species is shown in Fig. 3. The mean square radius of species 1 decreases, while that of species 2 increases.

The late-time density profiles of the two species ($t = 0.02R^2/\gamma$) are shown in Fig. 4. They compare well to the theoretical profiles predicted by Eqs. (61) and (63), shown by the dashed lines:

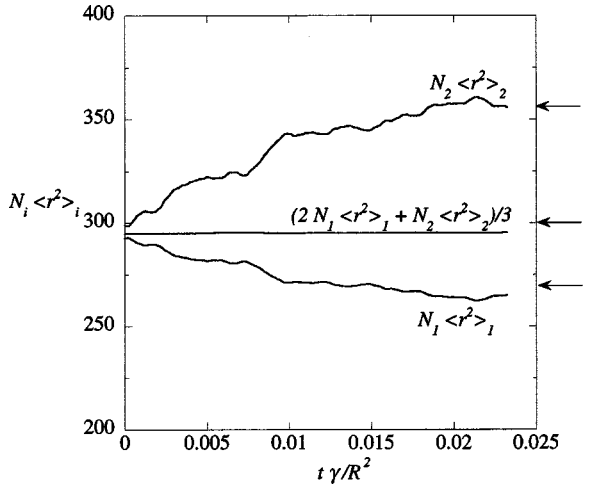

FIG. 3. Evolution of mean square radius in a molecular dynamics simulation of a two species point vortex gas with circulations γ and $\gamma/2$. The quantity $2N_1\langle r^2\rangle_1 + N_2\langle r^2\rangle_2$, which is theoretically exactly conserved, is also plotted. Arrows provide the theoretical equilibrium values for each quantity.

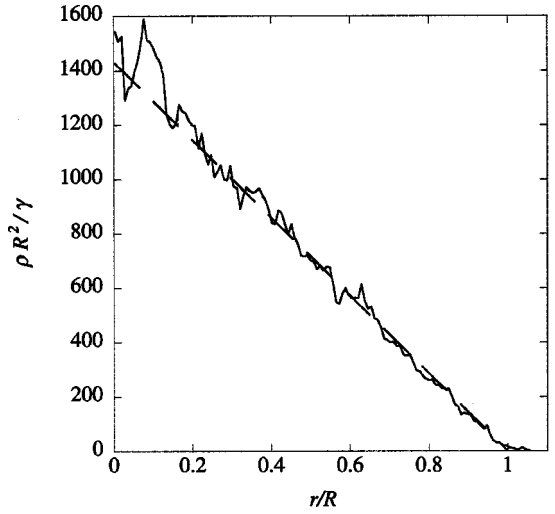

FIG. 5. Overall vorticity/charge density at the end of the run (solid) together with the initial vorticity density (dashed line).

$$\zeta_2(r) = \frac{-1+\sqrt{1+4C_1\rho(r)}}{2C_1},$$
$$\zeta_1(r) = C_1\zeta_2^2(r), \tag{67}$$

with $C_1 = 12.824\pi R^2/N\gamma$, chosen so that

$$N_1 = 2\pi \int r\ \ \zeta_1(r)dr/\gamma_1$$
$$= N_2 = 2\pi \int r\ \ \zeta_2(r)dr/\gamma_2 = 1000. \tag{68}$$

On the other hand, Fig. 5 shows that the total charge density has remained nearly unchanged, indicating that almost no viscous evolution toward a rigid-rotor thermal equilibrium has yet taken place.

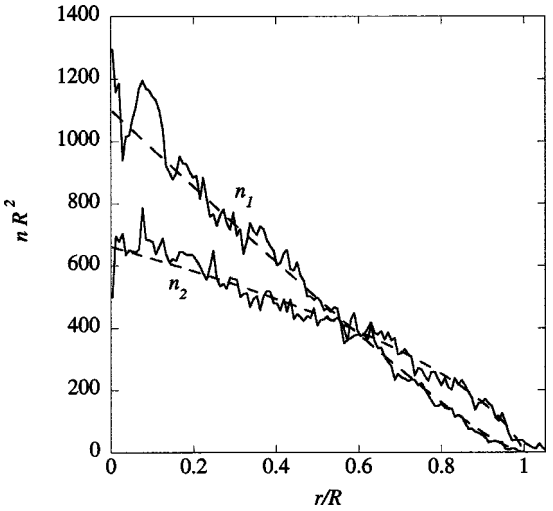

FIG. 4. Density profiles at the end of the molecular dynamics run. Also shown as dashed lines are the theoretical equilibrium profiles given by Eq. (66).

IV. DISCUSSION

In this paper we have calculated diffusion coefficients for a two-dimensional point vortex gas, or equivalently a two-dimensional guiding center plasma, in the presence of shear in the fluid velocity. The diffusion is reduced as the shear increases. When several species of point vortex are present, the diffusion causes vortices with relatively large circulation to concentrate at the peaks in the vorticity profile. This concentration is a statistical version of the motion of a single vortex up a vorticity gradient, a well-known phenomenon in fluid mechanics.[13,14]

There are several outstanding issues remaining. First, we found that although diffusive fluxes increase the entropy of the system, they do not cause the overall vorticity to vary in time. Viscous fluxes are required in order for the system to fully relax to a thermal equilibrium state. However, it has previously been shown that for a monotonically decreasing vorticity profile, the viscous fluxes vanish, at least when a quasilinear Klimontovitch approach is used in their calculation.[12] In order to understand viscous relaxation in this system, we must go beyond the quasilinear approach.

Second, the quasilinear and Boltzmann methods used here to calculate D_{ab}^{total} work only for retrograde flows, where $(\gamma_a+\gamma_b)S<0$. It has previously been shown for the prograde case, $(\gamma_a+\gamma_b)S>0$, that diffusion is considerably reduced compared to the retrograde case with the same value of $|S|$. This effect can be seen in the simulation results presented in Fig. 2 and is caused by vortices becoming trapped through their mutual interaction, as shown by the streamlines in Fig. 1(b).[9] No rigorous theory has been developed which can explain this reduction of diffusion in detail. One possible approach might be to employ Eq. (59), which relates diffusion to the drift velocity of vortices up or down the vorticity gradient in a second species. A ''mix and move'' estimate has been put forward for the drift velocity[13] of a species a vortex in a background of species b, in the case of prograde flow for which $|\gamma_a| \gg |\gamma_b|$, giving

$$v_{r_a} = -\frac{\gamma_a}{8\pi^2|S|}\frac{\partial \zeta_b}{\partial r}. \tag{69}$$

Using Eq. (59), this would imply that for prograde flow the off-diagonal diffusion coefficient is

$$\overline{D}^K_{ab} = \frac{\gamma_a \zeta_a}{8\pi^2|S|}, \tag{70}$$

and Eq. (58) would then imply

$$D^K_{ab} = \frac{\gamma_b \zeta_b}{8\pi^2|S|}. \tag{71}$$

This result for prograde flow is smaller than the retrograde result, Eq. (29), by the factor $[2\pi^2 \ln(r/d)]^{-1}$. However, it remains to be seen whether this reduction in diffusion actually explains the reduction observed in simulations of prograde flow. For prograde flow where $\gamma_a = \gamma_b$, Eq. (71) actually underestimates the diffusion by an order of magnitude (see the dotted line in Fig. 2); but this may be because Eq. (69) is only valid for $|\gamma_a| \gg |\gamma_b|$. More simulations (and, we hope, experiments) of systems with $|\gamma_a| \gg |\gamma_b|$ will be required in order to test the validity of Eqs. (70) and (71), and a theory valid for $|\gamma_a| \approx |\gamma_b|$ is still required.

Finally, we observe that the results of this paper only apply when the shear is strong enough to destroy the Dawson–Okuda vortices that are present at zero shear. The resonance-broadening approach used in Appendix A allows us to extend the results into the low-shear regime of $|S|r^2/D^{\text{total}} < 1$, but these results only qualitatively reproduce the Taylor–McNamara limit given by Eq. (2). Furthermore, in this low-shear regime a theory based on a local diffusion coefficient is not rigorously valid, since neither the correlation time nor the correlation length of the fluctuations are small.[23] Since experiments on nonneutral plasmas can probe this low-shear regime,[19] it is important to obtain accurate results for the diffusive flux due to Dawson–Okuda vortices in a cylindrical vortex patch. Theoretical investigations of this problem are currently underway.

ACKNOWLEDGMENTS

The author has benefitted from useful conversations with Professor C. F. Driscoll and Dr. F. Anderegg.

This research was suported by National Science Foundation Grant No. PHY-9876999 and Office of Naval Research Grant No. N00014-96-1-0239.

APPENDIX A: CALCULATION OF THE LOGARITHMIC CUTOFF VIA RESONANCE-BROADENING THEORY

In Sec. III we presented results for diffusion due to multiple simultaneous long-range collisions between point vortices. The theory was based on integration along unperturbed orbits as the vortices are carried along by the shear flow through the fluctuations. However, we found that the diffusion was dominated by interactions between nearby vortices, resulting in a logarithmic divergence that was cutoff by the diffusion itself, on a spatial separation scale δ: see Eq. (30). In this appendix we improve the theory so that no *ad hoc* cutoff need be introduced. This is accomplished by accounting for the diffusion in the orbit integrals, using resonance broadening theory. The result has the added benefit that it qualitatively reproduces the Taylor–McNamara result, Eq. (2), in the limit of zero shear. Thus, the resonance-broadening theory allows us to predict the diffusion for any value of the shear rate S.

We will consider only radial diffusion, and work in Cartesian coordinates (x,y) for simplicity, where x corresponds to the local radial direction and y corresponds to the local θ direction. Now the shear flow has the form $v_0(x)\hat{y}$ with shear rate $S = \partial v_0/\partial x$.

In these coordinates, the Kubo formula for the radial diffusion coefficient D^K is

$$D^K = \int_0^\infty dt \langle \delta v_x(t)\, \delta v_x(0)\rangle. \tag{A1}$$

The velocity fluctuations in the x direction are provided by Eq. (22), which when Fourier transformed yields

$$D^K = \sum_{p=1}^{N}\sum_{\overline{p}=1}^{N} \int_0^\infty dt\ \gamma_p \gamma_{\overline{p}} \int \frac{d^2k\, d^2\overline{k}}{(2\pi)^4}(-)\frac{k_y \overline{k}_y}{k^2 \overline{k}^2} \times \langle e^{i\mathbf{k}\cdot(\mathbf{r}(t)-\mathbf{r}_p(t))} e^{i\overline{\mathbf{k}}\cdot(\mathbf{r}(0)-\mathbf{r}_{\overline{p}}(0))}\rangle. \tag{A2}$$

Now the trajectory $\mathbf{r}_p(t)$ for each vortex is no longer specified by Eq. (24). Rather, we include the effect of diffusion in these orbits by adding random velocity fluctuations:

$$x_p(t) = \int_0^t dt\ \delta v_{x_p}(t) + x_{p_0},$$

$$y_p(t) = \int v_0(x_p(t))dt + y_{p_0} + \int_0^t dt\ \delta v_{y_p}(t) \approx v_0(x_{p_0})t + S\int_0^t dt' \int_0^{t''} dt'\ \delta v_{xp}(t') + y_{po} + \int_0^t dt\ \delta v_{yp}(t). \tag{A3}$$

In principle these velocity fluctuations should also be evaluated using Eq. (21). However, the averaging in Eq. (A2) then becomes too complex. Rather, we will assume that these fluctuations are uncorrelated white noise with Gaussian statistics such that $\langle \delta v_x \delta v_y\rangle = 0$, and $\langle \delta v_x(t)\, \delta v_x(t')\rangle = \langle \delta v_y(t)\, \delta v_y(t')\rangle = 2D^K \delta(t-t')$. Then the average in Eq. (A2) implies that only terms with $p = \overline{p}$ survive, and the expression becomes

$$D^K=\sum_a \gamma_a^2\int_0^\infty dt\int\frac{d^2k\,d^2\overline{k}}{(2\pi)^4}\int d^2r_{p_0}\,n(x_{p_0})e^{i(\mathbf{k}+\overline{\mathbf{k}})\cdot(\mathbf{r}_0-\mathbf{r}_{p_0})+ik_y[v_0(x_0)-v_0(x_{p_0})]t}(-)\frac{k_y\overline{k_y}}{k^2\overline{k^2}}$$
$$\times\left\langle e^{ik_x\int_0^t dt[\delta v_x(t)-\delta v_{x_p}(t)]+ik_y\{\int_0^t dt[\delta v_y(t)-\delta v_{y_p}(t)]+S\int_0^t dt''\int_0^{t''}dt'[\delta v_x(t')-\delta v_{x_p}(t')]\}}\right\rangle. \tag{A4}$$

The average over the white noise fluctuations can be carried out by first writing the integrals as Riemann sums, then using the uncorrelated nature of the statistics. For instance,

$$\left\langle e^{ik_y\int_0^t dt'\,\delta v_y(t')}\right\rangle=\Pi_{n=1}^{t/\Delta t}\int_{-\infty}^{\infty}d\delta v_{y_n}\frac{e^{-\frac{\delta v_{y_n}^2}{2\overline{v^2}}}}{\sqrt{2\pi\overline{v^2}}}e^{ik_y\sum_{n=1}^{t/\Delta t}\Delta t\,\delta v_{y_n}}, \tag{A5}$$

where $\overline{v^2}=2D^K/\Delta t$, $\delta v_{y_n}=\delta v_y(n\Delta t)$, and a Gaussian distribution for the fluctuations is assumed. After completing the squares in the integrals, the result is

$$\left\langle e^{ik_y\int_0^t dt'\,\delta v_y(t')}\right\rangle=e^{-k_y^2t\Delta t\overline{v^2}/2}=e^{-k_y^2D^Kt}. \tag{A6}$$

Equation (A4) then becomes

$$D^K=\sum_a\gamma_a^2n_a\int_0^\infty dt\int\frac{d^2k\,d^2\overline{k}}{(2\pi)^4}\int d^2r_{p_0}\,n_a(x_{p_0})$$
$$\times e^{i(\mathbf{k}+\overline{\mathbf{k}})\cdot(\mathbf{r}_0-\mathbf{r}_{p_0})+ik_y[v_0(x_0)-v_0(x_{p_0})]t}$$
$$\times(-)\frac{k_y\overline{k_y}}{k^2\overline{k^2}}e^{-2k^2D^Kt-2k_xk_yD^KSt^2-2k_y^2D^KS^2t^3/3}. \tag{A7}$$

For $D^K/(r_0^2S)\ll 1$, the integral over position x_{p_0} is dominated by $x_{p_0}\approx x_0$. Therefore we can expand: $v_0(x_0)-v_0(x_{p_0})\approx S(x_0-x_{p_0})$. We can now perform the integrals over $\mathbf{r}_{p_0}$ and $\overline{\mathbf{k}}$, yielding

$$D^K=\sum_a\gamma_a^2n_a(x_0)\int_0^\infty dt\int\frac{d^2k}{(2\pi)^2}\frac{k_y^2}{k^2((k_x+k_ySt)^2+k_y^2)}$$
$$\times e^{-2k^2D^Kt-2k_xk_yD^KSt^2-2k_y^2D^KS^2t^3/3}. \tag{A8}$$

If we set $D^K=0$ on the right-hand side of Eq. (A8), the integrals over t and k_x can be performed easily, yielding

$$D^K=\sum_a\frac{\gamma_a^2n_a(x_0)}{8|S|}\int\frac{dk_y}{|k_y|}. \tag{A9}$$

At small wave numbers the logarithmic divergence is cutoff at $k_{\min}=1/r_0$, since the y (i.e., θ) direction is periodic with period $2\pi r_0$. At large wave numbers the cutoff is at $k_{\max}=2\pi/\delta$, where $\delta=[4D^K/|S|]^{1/2}$. Equation (A9) then returns to Eq. (29).

If we keep finite D^K in Eq. (A8), the divergence at large k_x is regularized. In the limit as $S\to 0$, the integrals can be easily performed, yielding

$$D^K=\sum_a\frac{\gamma_a^2n_a(x_0)}{2D^K}\int\frac{d^2k}{(2\pi)^2}\frac{k_y^2}{k^6}$$
$$=\sum_a\frac{\gamma_a^2n_a}{2D^K}\frac{1}{(2\pi)^2}\frac{3\pi}{4}\int_{k_{\min}}^\infty\frac{dk_y}{k_y^3}.$$

Performing the integral and taking $k_{\min}=1/r_0$ implies

$$D_K^2=\sum_a\frac{\gamma_a^2n_a}{2}\frac{3r_0^2}{32\pi}. \tag{A10}$$

This result can only be regarded as approximate because we made the local approximation that the x_{p_0} integral in Eq. (A7) is dominated by $x_{p_0}\simeq x_0$, which is not true for zero shear. Nevertheless, Eq. (A10) does reproduce the expected Taylor–McNamara scaling that $D^K\sim\gamma\sqrt{N}$, at least for $r_0\approx R$. In order to do a better job for zero shear we must go beyond the resonance-broadening approach used here. This is a subject to which we will return in future work.

When both S and D^K are nonzero, the local approximation is valid and the integrals in Eq. (A8) can be performed in terms of special functions. First we add the periodicity cutoff $k_{\min}=1/r_0$ to the k_y integral, and we then change variables, taking $u=\sqrt{2D^K|S|}k_yt$, $v=\sqrt{2D^K/|S|}k_x+u/2$, and $\overline{k_y}=\sqrt{2D^K/|S|}k_y$. Then Eq. (A8) becomes

$$D^K=\sum_a\frac{\gamma_a^2n_a(x_0)}{(2\pi)^2}\frac{2}{|S|}\int_0^\infty du$$
$$\times\int_{\sqrt{(2D^K/|S|)}/r_0}^\infty d\overline{k_y}|\overline{k_y}|e^{-(u/|\overline{k_y}|)[\overline{k_y^2}+u^2/12]}$$
$$\times\int_{-\infty}^\infty\frac{dv\,e^{-uv^2/|\overline{k_y}|}}{[\overline{k_y^2}+(v-u/2)^2][\overline{k_y^2}+(v+u/2)^2]}. \tag{A11}$$

The integral over v can be evaluated in terms of error functions. If we define

$$g(\overline{k_y})=i\pi\overline{k_y}\int_0^\infty\frac{du}{u}e^{(u/\overline{k_y})(2\overline{k_y^2}-u^2/2)}$$
$$\times\left[\frac{e^{(u/\overline{k_y})[i\overline{k_y}+(u/2)]^2}}{\sqrt{(iu+2\overline{k_y})^2}}\mathrm{erfc}\left[\frac{\sqrt{(iu+2\overline{k_y})^2u/\overline{k_y}}}{2}\right]\right.$$
$$\left.-\frac{e^{(u/\overline{k_y})[i\overline{k_y}-(u/2)]}}{\sqrt{(iu-2\overline{k_y})^2}}\mathrm{erfc}\left[\frac{\sqrt{(iu-2\overline{k_y})^2u/\overline{k_y}}}{2}\right]\right] \tag{A12}$$

then Eq. (A11) becomes

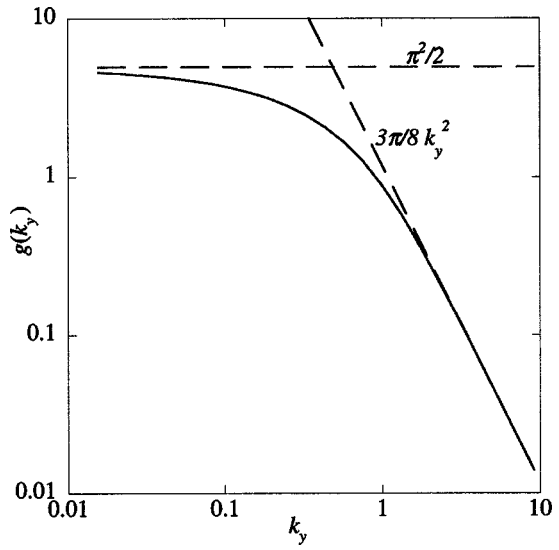

FIG. 6. The function $g(\bar{k}_y)$ appearing in Eq. (A13).

$$D^K=\sum_a \frac{\gamma_a^2 n_a(x_0)}{(2\pi)^2}\frac{2}{|S|}\int_{\sqrt{(2D^K/|S|)}/r_0}^{\infty} d\bar{k}_y \frac{g(\bar{k}_y)}{\bar{k}_y}. \quad \text{(A13)}$$

A plot of $g(\bar{k}_y)$ is shown in Fig. 6. As $\bar{k}_y \to 0$, one can show that $g \to \pi^2/2$. Also at large $\bar{k}_y$, one can show that $g \to 3\pi/8\bar{k}_y^2$, so the integral in Eq. (A13) is not divergent. In the limit that $\sqrt{2D^K/|S|}r_0 \ll 1$, Eq. (A13) becomes

$$D^K=\sum_a \frac{\gamma_a^2 n_a}{(2\pi)^2}\frac{2}{|S|}\frac{\pi^2}{2}\ln(\alpha r_0/\sqrt{2D^K/|S|}), \quad \text{(A14)}$$

where α is a number of order unity. This reproduces the logarithmic cutoff previously introduced in an *ad hoc* fashion in Eq. (29). The value of α, found numerically by evaluating the integral in Eq. (A13), is $\alpha \approx 1/4$.

APPENDIX B: ONSAGER RELATIONS FOR DIFFUSION IN A POINT VORTEX GAS

The continuity equation for the vorticity of species a may be written as

$$\frac{\partial \zeta_a}{\partial t}=-\nabla\cdot\mathbf{J}_a, \quad \text{(B1)}$$

where $\mathbf{J}_a$ is the vorticity flux. According to Onsager,[24] the vorticity flux caused by diffusion can be expressed in the following manner:

$$\mathbf{J}_a=\sum_b L_{ab}\nabla X_b, \quad \text{(B2)}$$

where $X_b=\partial\mathcal{S}/\partial\zeta_b$, $\mathcal{S}$ is the entropy density of the gas, and where L_{ab} are symmetric transport coefficients satisfying $L_{ab}=L_{ba}$. For an ideal gas of point vortices, the entropy density is

$$\mathcal{S}=-\sum_b \frac{\zeta_b}{\gamma_b}\ln\zeta_b \quad \text{(B3)}$$

[see Eq. (62)] which implies that $X_b=-(1/\gamma_b)(\ln\zeta_b+1)$. Therefore, we can write Eq. (B1) as

$$\frac{\partial \zeta_a}{\partial t}=\sum_b \nabla\cdot\bar{D}_{ab}\nabla\zeta_b, \quad \text{(B4)}$$

where

$$\bar{D}_{ab}=\frac{L_{ab}}{\gamma_b\zeta_b}. \quad \text{(B5)}$$

Since $L_{ab}=L_{ba}$,

$$\bar{D}_{ba}=\frac{L_{ba}}{\gamma_a\zeta_a}=\frac{L_{ab}}{\gamma_a\zeta_a}=\frac{\gamma_b\zeta_b}{\gamma_a\zeta_a}\bar{D}_{ab}, \quad \text{(B6)}$$

proving Eq. (58).

APPENDIX C: ENTROPY PRODUCTION FROM DIFFUSION

In this appendix we derive an expression for the rate of entropy production due to the diffusive flux given by Eq. (55). This expression shows explicitly that entropy increases in the diffusive rearrangement of multiple charge species.

Starting with Eq. (62) for the entropy $\mathcal{S}$, we take a time derivative and apply Eq. (46) to obtain

$$\frac{d\mathcal{S}}{dt}=\sum_a \frac{1}{\gamma_a}\int d^2r\frac{1}{r}\frac{\partial}{dr}(r\ J_{r_a})[\ln\zeta_a+1]. \quad \text{(C1)}$$

Integrating by parts, and substituting for J_{r_a} from Eq. (55) yields

$$\frac{d\mathcal{S}}{dt}=\sum_a\sum_b\int d^2r\left[D_{ab}^K\frac{\partial\zeta_a}{\partial r}-\bar{D}_{ab}^K\frac{\partial\zeta_b}{\partial r}\right]\frac{1}{\gamma_a\zeta_a}\frac{\partial\zeta_a}{\partial r}. \quad \text{(C2)}$$

Expressing D_{ab}^K and $\bar{D}_{ab}^K$ in terms of the symmetric Onsager transport coefficient L_{ab} via Eqs. (B5) and (57), Eq. (C2) becomes

$$\frac{d\mathcal{S}}{dt}=\sum_a\sum_b\int d^2r\,L_{ab}\left[\frac{\gamma_b\zeta_b}{\gamma_a\zeta_a}\left(\frac{\partial\zeta_a}{\partial r}\right)^2-\frac{\partial\zeta_a}{\partial r}\frac{\partial\zeta_b}{\partial r}\right]. \quad \text{(C3)}$$

Finally, applying the Onsager relation $L_{ab}=L_{ba}$, Eq. (C3) can be written as

$$\begin{aligned}\frac{d\mathcal{S}}{dt}&=\frac{1}{2}\sum_{ab}\int d^2r\,L_{ab}\left[\frac{\gamma_b\zeta_b}{\gamma_a\zeta_a}\left(\frac{\partial\zeta_a}{\partial r}\right)^2\right.\\&\left.\quad+\frac{\gamma_a\zeta_a}{\gamma_b\zeta_b}\left(\frac{\partial\zeta_b}{\partial r}\right)^2-2\frac{\partial\zeta_a}{\partial r}\frac{\partial\zeta_b}{\partial r}\right]\\&=\frac{1}{2}\sum_{ab}\int d^2r\frac{L_{ab}}{\gamma_a\zeta_a\gamma_b\zeta_b}\left[\gamma_b\zeta_b\frac{\partial\zeta_a}{\partial r}-\gamma_a\zeta_a\frac{\partial\zeta_b}{\partial r}\right]^2. \quad \text{(C4)}\end{aligned}$$

This expression implies $d\mathcal{S}/dt \geqslant 0$, with equality only when the square brackets vanish. However, Eqs. (55) and (57) imply that this condition is equivalent to the equilibrium condition $J_{r_a}=0$.

[1]For a review see P.G. Saffmann and G.R. Baker, Annu. Rev. Fluid Mech. **11**, 95 (1979).
[2]L. Onsager, Nuovo Cimento, Suppl. **6**, 279 (1949).
[3]G.F. Carnevale, J.C. McWilliams, Y. Pomeau, J.B. Weiss, and W.R. Young, Phys. Rev. Lett. **66**, 2735 (1991).
[4]Y.P. Pointin and T.S. Lundgren, Phys. Fluids **19**, 1459 (1976).
[5]R.H. Kraichnan, J. Fluid Mech. **67**, 155 (1975).
[6]G. Joyce and D. Montgomery, J. Plasma Phys. **10**, 107 (1973).
[7]J.B. Taylor and B. McNamara, Phys. Fluids **14**, 1492 (1971).
[8]J.M. Dawson, H. Okuda, and R.N. Carlile, Phys. Rev. Lett. **27**, 491 (1971).
[9]D.H.E. Dubin and D.Z. Jin, Phys. Lett. A **284**, 112 (2001).
[10]K.H. Burrell, Phys. Plasmas **4**, 1499 (1997).
[11]R.H. Levy, Phys. Fluids **8**, 1288 (1965); **11**, 920 (1968).
[12]D.H.E. Dubin and T.M. O'Neil, Phys. Rev. Lett. **60**, 1286 (1988).
[13]D.A. Schecter and D.H.E. Dubin, Phys. Rev. Lett. **83**, 2191 (1999).
[14]C.G. Rossby, J. Mar. Res. **1**, 175 (1948).
[15]D.A. Schecter and D.H.E. Dubin, Phys. Fluids **13**, 1704 (2001).
[16]P.H. Chavanis, Phys. Rev. Lett. **84**, 5512 (2000).
[17]R. Robert and J. Sommeria, Phys. Rev. Lett. **69**, 2776 (1992).
[18]P.H. Chavanis, Phys. Rev. E **64**, 026309 (2001).
[19]C.F. Driscoll, Phys. Plasmas **9**, 1905 (2002).
[20]L.E. Reichl, *A Modern Course in Statistical Physics* (University of Texas Press, Austin, 1980), p. 528.
[21]See Ref. 20, p. 527.
[22]P.B. Rhines, J. Fluid Mech. **69**, 417 (1975).
[23]J.A. Krommes and C. Oberman, J. Plasma Phys. **16**, 229 (1976).
[24]See Ref. 20, p. 509.